Cardiac investigations in sudden unexpected death in DEPDC5 -related epilepsy

Alexandre Bacq, Delphine Roussel, Thomas Bonduelle, Sara Zagaglia, Marina Maletic, Théo Ribierre, Homa Adle-Biassette, Cécile Marchal, Mélanie Jennesson, Isabelle An, et al.

Cardiac investigations in sudden unexpected death in DEPDC5-related epilepsy

Running head: Cardiac investigations in Depdc5-related SUDEP

Alexandre Bacq[1], Delphine Roussel[1], Thomas Bonduelle[1,2], Sara Zagaglia[3], Marina Maletic[1], Théo Ribierre[1], Homa Adle-Biassette[4], Cécile Marchal[2], Mélanie Jennesson[5], Isabelle An[6], Genomics England Research Consortium*, Fabienne Picard[7], Vincent Navarro[1,6], Sanjay M Sisodiya[3] and Stéphanie Baulac[1]

Affiliations:

[1] Sorbonne Université, Institut du Cerveau - Paris Brain Institute - ICM, Inserm, CNRS, APHP, Hôpital de la Pitié Salpêtrière, F-75013, Paris, France

[2] Service épilepsie et neurologie, CHU de Bordeaux, Bordeaux, France

[3] UCL Queen Square Institute of Neurology, London WC1N 3BG, and Chalfont Centre for Epilepsy, Bucks, UK

[4] Université de Paris, service d'Anatomie Pathologique, AP-HP, Hôpital Lariboisière, DMU DREAM, UMR 1141, INSERM, Paris, France

[5] CHU Reims, American Memorial Hospital, Service de Pédiatrie, Reims, F-51092, France

[6] AP-HP, Pitié-Salpêtrière Hospital, Epileptology Unit and Reference Center of Rare Epilepsies, Paris, France

[7] EEG and Epilepsy Unit, Department of Clinical Neurosciences, University Hospitals and Faculty of Medicine of Geneva, Geneva, Switzerland

* Genomics England Research Consortium contributors are listed in Supplementary Table 1

Correspondence to: Stéphanie Baulac, PhD

Institut du Cerveau (ICM) - Paris Brain Institute
Hôpital Pitié-Salpêtrière - 47, bd de l'hôpital - 75013 Paris
Phone : +33 (0)1 57 27 43 39 / E-mail: stephanie.baulac@icm-institute.org

Abstract

Objective: Germline loss-of-function mutations in *DEPDC5*, and in its binding partners (*NPRL2/3*) of the mTOR repressor GATOR1 complex, cause focal epilepsies and increase the risk of sudden unexpected death in epilepsy (SUDEP). Here, we asked whether *DEPDC5* haploinsufficiency predisposes to primary cardiac defects that could contribute to SUDEP and therefore impact the clinical management of patients at high risk of SUDEP. **Methods:** Clinical cardiac investigations were performed in sixteen patients with pathogenic variants in *DEPDC5*, *NPRL2* or *NPRL3*. Two novel Depdc5 mouse strains, a HA-tagged Depdc5 mouse strain and a Depdc5 heterozygous knockout with a neuron-specific deletion of the second allele (*Depdc5*$^{c/-}$) were generated to investigate the role of Depdc5 in SUDEP and cardiac activity during seizures. **Results:** Holter, echocardiography and ECG exams provided no evidence for altered clinical cardiac function in the patient cohort, of whom three *DEPDC5*-patients succumbed to a SUDEP and six had a family history of SUDEP. There was no cardiac injury at autopsy in a postmortem *DEPDC5*-SUDEP case. The HA-tagged Depdc5 mouse revealed expression of Depdc5 in the brain, heart and lungs. Simultaneous EEG-ECG records on *Depdc5*$^{c/-}$ mice showed that spontaneous epileptic seizures resulting in a SUDEP-like event, are not preceded by cardiac arrhythmia. **Interpretation:** Mouse and human data show neither structural nor functional cardiac damage that might underlie a primary contribution to SUDEP in the spectrum of DEPDC5-related epilepsies.

Keywords: mTOR pathway, epilepsy, SUDEP.

Abbreviations DEPDC5: Dishevelled, Egl-10 and Pleckstrin Domain Containing protein 5; FCD: focal cortical dysplasia; GATOR1: Gap-Activity Towards Rag complex 1; GTCS: generalized tonic-clonic seizure; NPRL2/3: Nitrogen-Permease Regulator Like 2/3; PGES: postictal generalized EEG suppression; SUDEP: sudden unexpected death in epilepsy; TTE: transthoracic echocardiography.

Introduction

Sudden unexpected death in epilepsy (SUDEP) is a tragic outcome which is the most common cause of epilepsy-related death[1], with an incidence of 1.2 per 1000 person-years in adults and 0.2 per 1000 person-years in children[2,3]. While the pathophysiological mechanisms of death in SUDEP are still unclear, three explanations predominate: a cerebral shutdown associated with a generalized tonic-clonic seizure (GTCS), an autonomic dysfunction, and/or a cardiorespiratory failure[4–7]. Cardiac dysfunction has received much attention since SUDEP shares features with sudden cardiac death[8–10]. Cardiac arrhythmia can be caused by mutations in ion channel genes: *SCN1A*, *KCNA1*, *KCNQ1* or *CACNA1A*[8–11] or by seizure-induced physiological changes[5,6,12,13]. Discriminating between the two hypotheses would have clinical implications, since genetic cardiac dysfunction leading to fatality may be preventable and indicate a need for cardiological surveillance in patients at high risk of SUDEP[14].

SUDEP was recently reported in epileptic patients with mutations in the non-ion channel epilepsy gene *DEPDC5*, as well as its binding partners *NPRL2* and *NPRL3*, that form the GATOR1 complex[15–18]. First reported in two individuals from the same family[15], *DEPDC5* variants were then found in 10% of 61 SUDEP cases in an exome-based study[16]. SUDEP was also reported in 10% of a cohort of 73 GATOR1-related families[17]. Furthermore, sudden death is observed in rodent models of *Depdc5*-deficiency[19–22]. How *DEPDC5* mutations may contribute to SUDEP is unknown. The GATOR1 complex is part of the amino-acid sensing branch which inhibits complex 1 of the mammalian target of rapamycin (mTOR) pathway[23]. In this complex, DEPDC5 is the central component which interacts directly with the Rags, to regulate mTORC1 activity[24]. The mTOR signaling pathway regulates key cellular functions promoting cell growth and metabolism in response to environmental cues including growth factors, hormones and nutritients[25]. Germline mutations in the *DEPDC5* gene are the most frequent cause of genetic focal epilepsies; mutations in *NPRL2* and *NPRL3* are also encountered, although more rarely[17,18,26–29]. GATOR1 mutations act typically as a loss-of-function leading to constitutive activation of the mTOR pathway, as observed in resected brain tissues from operated patients with refractory epilepsy and mouse models[18–22,30]. Recently, *DEPDC5* brain somatic second-hit mutations occurring on top of germline *DEPDC5* heterozygous mutations, have been shown to cause focal cortical dysplasia type 2 (FCD type 2), a localized cortical malformation manifesting with intractable epilepsy[19,30–33].

Preventive strategies to allay the risk of SUDEP in individuals with GATOR1 mutations require the identification of biomarkers to predict SUDEP susceptibility and understanding how seizures lead to death. Here, to test the hypothesis that mutations in *DEPDC5* (or in *NPRL2* and *NPRL3*) may induce primary cardiac alterations predisposing to SUDEP, we conducted cardiac investigations in a cohort of 16 GATOR1-patients and assessed by simultaneous EEG-ECG records cardiac-related

mechanisms in a novel mouse model of *Depdc5*-deficiency presenting with fatal spontaneous seizures, resembling SUDEP-like events.

Materials and methods

Study Approval

Written informed consent was obtained from all participants (French cohort: C14-56 GENEPI; UK cohort: 11/LO/2016). Mouse studies were approved by the French Ministry of Research (no. APAFIS#3506).

Cardiac investigation in patients

We enrolled a cohort of 16 patients with pathogenic mutations in *DEPDC5* (n=14), *NPRL2* (n=1) or *NPRL3* (n=1), among which six were previously reported[17,18]. Genetic testing was performed antemortem from genomic blood DNA. Results from cardiac and neurological investigations including patient history, physical examination, twelve-lead ECGs and in some cases Holter monitor and TTE records were collected retrospectively.

Brain and heart postmortem examination of a SUDEP case

Postmortem examination of heart and brain tissue from a patient with a *DEPDC5* mutation was conducted by an expert pathologist (H.A.B). Samples of different regions from whole fixed brain and heart were assessed using a comprehensive gross and histologic examination as previously performed[34].

Generation of *Depdc5* strain mice

Two mouse strains were generated by genOway on a C57BL6/J background: a mouse carrying an HA-tagged Depdc5 flanked by LoxP sequences at the endogenous locus of *Depdc5* and a heterozygous deletion of *Depdc5* termed *Depdc5*$^{+/-}$. The universal Cre-driver Synapsin1-Cre mouse (B6.Cg-Tg(Syn1-cre)671Jxm/J) was imported from the Jackson Laboratory.

Generation of Depdc5 HA-tagged and flox mice

HA-*Depdc5*$^{flox/flox}$ mice were generated by flanking exons 1-3 with LoxP sites and an HA tag in the N-terminal region. An HA-tag in the N-terminal part of Depdc5 was previously reported not to affect the protein interactions, and preserve the role of HA- as a repressor of mTORC1[23]. HA-*Depdc5*$^{flox/flox}$ mice are viable and show no gross physical differences from wild-type littermates. To simplify, we named HA-Depdc5 the mice having an HA-Tag.

Generation of Depdc5 conditional KO

Depdc5 conditional KO mice were generated by first breeding *Depdc5*$^{+/-}$ males and Syn1-Cre^{+} females to obtain *Depdc5*$^{+/-}$;Syn1-Cre^{+} mice. *Depdc5*$^{+/-}$;Syn1-Cre^{+} females were then crossed with *Depdc5*$^{flox/flox}$ males to generate four genotypes, among which three were used: *Depdc5*$^{c/-}$ conditional KO (*Depdc5*$^{flox/-}$;Syn1-Cre^{+}), *Depdc5*$^{+/-}$

constitutive heterozygous (*Depdc5*$^{flox/-}$;Syn1-Cre^{-}) and *Depdc5*$^{+/+}$ control wild-type (*Depdc5*$^{flox/+}$;Syn1-Cre^{-}). Genomic DNA was extracted from tail biopsies. All mice were genotyped by PCR at the iGenSeq sequencing facility of ICM. Three primer pairs were used to genotype *Depdc5* alleles: 2 forwards: CCTTTCAGCCGAACAACCACCAGT and GCACCAGAAGTCAGATCTCATTATGG and one reverse: GCTCTCATTTCCAACCATCCCTG. All breeding couples were previously back-crossed for > 10 generations into the C57BL/6J background.

Mice were housed in groups of 2-6 in standard plastic cages on a 12-h light/dark cycle under pathogen-free conditions at the ICM animal core facility. Animals implanted for EEG and ECG records were housed singly. Water and food were provided *ad libitum*. Animals were treated according to the guidelines of the European Community. All efforts were made to minimize the number and the suffering of animals. Both males and females were used in the study.

Western blots

Mouse organs were processed as previously described[35]. The following primary antibodies were used: rat anti-HA (1/1000, 3F10, Sigma), rabbit anti-Depdc5 (1/250, ab185565, abcam), rabbit anti-phospho-S6 Ribosomal Protein (1/500, 5364, Cell Signaling) and rabbit anti-α-actin antibody (1/1000, A2066, Sigma-Aldrich); secondary antibodies were: anti-rat HRP-linked (1/2000, 7077, Cell Signaling) and anti-rabbit peroxidase stabilized (1/2000, 32460, Invitrogen). Protein expression were quantified by densitometry using Fiji software and normalized against actin.

Immunohistochemistry

Adult (aged P85) mouse brains were collected after perfusion with 4% paraformaldehyde (PFA), as previously described[35]. All immunostainings were performed on sections from the somatosensory cortex, in duplicate in three sections per animal (n = 2 mice per genotype). Primary antibodies used were: rabbit anti-HA (1/1500, C29F4, Cell Signaling), mouse anti-NeuN (1/200, MAB377, Millipore), mouse anti-Map2 (1/500, ab11267, abcam), mouse anti-CamkII (1/500, ab22609, abcam), rat anti-LAMP1 (1/500, 1D4B, DSHB), goat anti-Gad67 (1/400, MAB5406, Millipore), mouse anti-PV (1/1000, P3088, Sigma), mouse anti-Gfap (1/300, MA5-15086, Thermofisher), rat anti-Plp (1/10, hybridoma), mouse anti-Olig2 (1/400, ab236540, abcam) and goat anti-Iba1 (1/500, 011-27991, WAKO). Secondary antibodies were: donkey anti-rabbit-alexa-555, anti-rat-alexa-488, anti-goat-alexa-488 and anti-mouse-alexa-488 (1/1000; Invitrogen A32794, A-21208, A32814 and A32766, respectively). Images were acquired using Zen software with an upright, widefield, apotome Zeiss microscope and a confocal Leica SP8 microscope. Quantification of colocalization was performed using JaCoP plugin in ImageJ software. The fraction of cell types expressing Depdc5 was assessed using ImageJ software (using automatic particle counting).

Adult (P85) mouse hearts were collected before seizure onset or after SUDEP and were fixed in PFA 4%. Transverse sections (20 µm) were cut and stained with

Hematoxilin-Eosin (HE) (n= 3 *Depdc5*$^{+/+}$ hearts, 3 *Depdc5*$^{c/-}$ hearts before seizures and 4 *Depdc5*$^{c/-}$ after SUDEP*)*.

Simultaneous EEG-ECG recordings

Two groups of mice were used: one for EEG recordings (n= 10 *Depdc5*$^{c/-}$, n= 7 *Depdc5*$^{+/+}$ and n= 3 *Depdc5*$^{+/-}$ mice); and one for simultaneous EEG-ECG recordings (n= 23 *Depdc5*$^{c/-}$ and n= 4 *Depdc5*$^{+/+}$ mice). Mice were anesthetized (2-4% isoflurane) under analgesia (0.1 mg/kg buprecare for 48h). EEG recording electrodes were implanted into mice placed in a stereotaxic frame. Home-made enamel-coated stainless-steel electrodes (A-M SYSTEMS, # 791400) were placed in primary motor cortex (Bregma: AP, 2.2 mm; MD, 2.2 mm) and the lateral parietal association cortex (Bregma: AP, -1.8 mm; MD, -1.2 mm). A bipolar electrode was placed in the left hippocampus (Bregma: AP, -1.8 mm; MD, -1.8 mm; DV, -1.8 mm) and a reference electrode on the cerebellum. Coordinates were derived and adjusted from the Paxinos and Watson atlas[36]. ECG records were obtained from two electrodes placed by tunneling subcutaneously, one in the right scapular region and the other in the left abdominal muscle[37]. After 1-week recovery period, implanted mice were permitted free movement, connected to an ADC amplifier (Brainbox EEG-1166) as part of an EEG-video acquisition system (Deltamed, Natus). EEG signals were acquired at 2 kHz and pass band filtered (0.5-70 Hz). Video was recorded at 25 frames/s, synchronized to electrophysiological signals. For the EEG group, recordings were made 24/24 over 4-6 consecutive days from P21 until P117, or until a fatal seizure; for the EEG-ECG group, recordings were made 24/24, 7/7 from P80 until a fatal seizure. Seizures were detected electrically as EEG spikes causing a rapid increase in signal amplitude and power analyzed over a sliding window of 20 s. Signal analysis for representative images was made using MATLAB (Mathworks). Morlet wavelets were computed from 0.5-45 Hz at a resolution of 0.1 Hz, over a sliding time window of 1 s, updated each 0.1 s. Events were detected on both time and frequency criteria. RR intervals were analyzed with Spike2 software, and heart rate was calculated as number of RR in 2s (Spike2 version 7.06; Cambridge Electronic Design).

Heart Rate Variability (HRV) was assessed by different parameters: SDRR (Standard Deviation of all RR), rMSSD (square root of mean of successive square differences between RR), and using Poincaré plots[38,39]. This later method graphs the time between one pair of QRS complexes on an ECG (RR) versus the time between the next pair of QRS complexes (RR'). The. SD1 and SD2 refer to short-term and long-term adaptation, respectively. For all Poincaré plots, more than 500 pairs of RR intervals were plotted and analyzed. Recordings during animal movements were excluded to eliminate artifacts.

ECG recordings in anesthetized mice

Mice (n=18) were used for this study (n=9 *Depdc5*$^{c/-}$ and n=9 *Depdc5*$^{+/+}$ mice) aged P80. The QRS component of the ECG was recorded from anesthetized mice (2-4% isoflurane) kept warm to 35-37°C with a heating pad. A specific ECG recording system

was used (ElectroMyography; Neurosoft) to amplify records made with a needle electrode (Technomed, TE/B50600-001) inserted subcutaneously near the heart. Ground signals were obtained from a needle electrode (Spesmedica, N3512P150) inserted into the back of the animal. Signals were band pass filtered (0.02-10 kHz) and analyzed with Spike2 software. RR interval length, PR, QT and QRS lengths were measured and SDRR and rMSSD were calculated.

Statistical analysis

The number of mice per group was as determined from the resource equation method to sample size and is indicated in each figure legend[40]. Normality distributions of data were tested with the Shapiro-Wilk normality test. Unpaired two-tailed t tests or Mann-Whitney tests were used to compare sets of data obtained from independent groups of animals (*Depdc5*$^{+/+}$ vs. *Depdc5*$^{c/-}$, or fatal vs. non-fatal groups). For survival, Log-rank test was performed. Two-way ANOVA test was performed for comparisons included more than two groups. All statistical analyses were performed with Prism 7 (Graphpad software Inc), as described in figure legends. Statistical significance was set at $\alpha < 0.05$.

Results

Cardiac investigations in the GATOR1 patient cohort

We explored cardiac function in subjects carrying mutations in GATOR1-encoding genes, suffering recurrent seizures. Table 1 presents the cohort which comprised patients with germline pathogenic nonsense variants in *DEPDC5* (n=14), *NPRL2* (n=1) or *NPRL3* (n=1). All patients were diagnosed with focal epilepsy (Table 2). Age at epilepsy onset ranged from 1- 27 years (mean: 8 years and 3 months). A family history of SUDEP was documented in six patients. Two females with *DEPDC5* mutations aged 18 and 50 (patients #1 and #2) and one male patient aged 20 (patient #16) had definite (1/3) and probable (2/3) SUDEP after they were recruited into the genetic study. Notably, two of these three patients (#1 and #2) were seizure-free for 8 months and 9 years before SUDEP.

Age at cardiac investigation ranged from 16-60 years (mean: 39 years and 9 months, Table 3). Individual #11 (with family history of SUDEP) had a history of recurrent syncopal episodes, unrelated to epilepsy and most likely due to autonomic origin as orthostatic intolerance was diagnosed. In the cohort, no abnormal heart sounds were detected in cardiac auscultations. Twelve-lead ECG monitoring revealed PR, QRS and QTc intervals that fell within normal ranges in 14/16 patients (87.5%), except for one *NPRL3* subject (#6) and one *DEPDC5* subject (#10) who presented with an isolated incomplete right bundle branch block. No ST-segment changes were evident indicating normal ventricular repolarization. One patient (#12) showed borderline left axis deviation and subtle T abnormalities, with normal QTc and PR intervals. In the context of presurgical evaluation of patient #12, the video-EEG-ECG telemetric system

captured four episodes of ictal bradycardia with heart rate down to 42 bpm, which were followed with post-ictal HR normalization. Holter monitoring for 24 hours to 8 continuous days revealed no major cardiac arrhythmias in 4/4 patients including three (patients #5, #6 and #13) with a family history of SUDEP. Two-dimensional TTE excluded any major structural or functional heart disease in 6/6 patients. Most patients (14/16) received sodium channel blockers as antiepileptic medication (Table 2), among which the three patients who died from SUDEP. Overall, these data provide no evidence that baseline cardiac parameters can accurately predict sudden death in patients with GATOR1 pathogenic variants, including in high-risk patients who have a family history of SUDEP.

Postmortem cardiac examination of a SUDEP *DEPDC5* case

Patient #1 had nonlesional sleep-hypermotor epilepsy (SHE) since the age of 7 years; seizures responded well to carbamazepine from the age of 9 years. She carried a paternally inherited germline pathogenic *DEPDC5*: c.2620C>T/p.Arg874* variant. SUDEP was suspected in the sudden death of her paternal granduncle after a diurnal seizure. No specific anomalies were detected in the ECG and TTE examinations that were performed at the age of 16 years in the context of a possible familial SUDEP history (Tables 1,3). At the age of 18, patient #1 died during sleep. A probable seizure that night was identified on questioning the family (noise of convulsive movements), even though the patient had been seizure-free on carbamazepine for 9 years.

Possible medical causes of unnatural death, including illicit drug use, were excluded. Definite SUDEP was confirmed following autopsy, which included the heart and brain examination, and did not reveal any abnormalities. The heart weighed 279g. Histological examination of mapped, labelled blocks of myocardium from representative transverse slices of both ventricles was performed (Fig. 1A-E). No lesions were identified in the coronary arteries, the myocardium or the cardiac valves. No ischemic sequelae, thrombus, fibrosis or scars were evident. Moreover, we did not detect contraction band necrosis, a common finding in neurocardiac death (Fig. 1C-E)[41]. Brain autopsy was also performed. The brain weighed 1630 g, which is 2.5 standard deviations above the average for age and gender, suggesting macrocephaly. Macroscopic examination excluded contributions of any other major cerebral injury to the SUDEP.

There was no evidence for primary cardiac dysfunction leading to SUDEP in this *DEPDC5* case. To further investigate the role of DEPDC5 in SUDEP pathomechanism, we generated mice models of *Depdc5* haploinsufficiency.

Depdc5 spatio-temporal expression pattern

While interest in the *DEPDC5* epilepsy gene has tremendously increased, the pattern of expression of Depdc5 protein remains unclear, since no specific antibody is available. To provide this missing information, we generated a mouse strain expressing an endogenous version of Depdc5 HA-tagged at the N-terminus. Western blot with an anti-HA tag antibody detected specific high expression levels of the HA-Depdc5 in the

brain, moderate levels in the heart, lungs, muscle, skin and adipose tissue, but there was little or no expression in liver or kidneys (Fig. 2A). During development, brain HA-Depdc5 expression was apparent from embryonic day 10 (E10) and levels increased until they reached a stable expression from P21 to adulthood (Fig. 2B). In adult mice, HA-Depdc5 was detected in all brain regions examined including cortex, hippocampus, striatum, septum, olfactory bulb, thalamus-hypothalamus, cerebellum and brainstem (Fig. 2C). We next assessed which cortical cell subtypes express Depdc5. HA staining was specific when comparing HA-Depdc5 cortical slices to wild-type untagged (Fig. 2D-E). All NeuN-positive neurons expressed HA-Depdc5 (Fig. 2D), particularly in the soma (see insets of Fig. 2D), where it colocalizes with the lysosomal marker Lamp1 (Fig. 2E; Pearson's coefficient = 0.49 corresponding to a moderate/high colocalization). HA-Depdc5 was also detected in both proximal and distal MAP2-positive dendrites, as shown in mouse primary cortical neuron cultures (Fig. 2F). HA-Depdc5 was detected in both excitatory (CaMKII-positive) and inhibitory (Gad67- and PV-positive) cortical neurons (Fig. 2G) but not in glial cells (identified by Gfap immunostaining for astrocytes, Olig2 and Plp for oligodendrocytes, and Iba1 for microglia; Fig. 2H).

In summary, Depdc5 protein is most highly expressed in the brain, and moderately in the heart and the lungs. To assess cardiac activity during seizures, we next generated a novel mouse model of *Depdc5*-deficiency.

Spontaneous seizures and SUDEP in *Depdc5*$^{c/-}$ mice

To model the human genetic condition, we generated a heterozygous *Depdc5*$^{+/-}$ mouse and deleted the second *Depdc5* allele specifically in neurons (using a Synapsin1-driven Cre recombinase in *Depdc5* flox strain), termed *Depdc5*$^{c/-}$ (see Fig. 3A and methods for details). We confirmed both a significant reduction of brain Depdc5 expression and a robust increase in mTOR signaling in *Depdc5*$^{c/-}$ mice, measured with the phosphorylation level of the downstream target ribosomal protein S6 (pS6) by Western blot (Fig. 3B). *Depdc5*$^{c/-}$ mice were born in the expected Mendelian ratio, with no obvious morphological differences from wild-type littermates (*Depdc5*$^{+/+}$). However, the lifespan of *Depdc5*$^{c/-}$ mice was much reduced compared to *Depdc5*$^{+/+}$ littermates. No *Depdc5*$^{c/-}$ mice survived after 140 days (median 103 days, Fig. 3C), while WT *Depdc5*$^{+/+}$ all survived beyond 200 days of age. Spontaneous behavioral seizures were often observed in adult *Depdc5*$^{c/-}$ mice. Eventually all *Depdc5*$^{c/-}$ mice were found dead in a tonic posture presumably after an epileptic seizure, suggesting a SUDEP-like event. To confirm this hypothesis, cortical and hippocampal EEG electrodes were implanted in *Depdc5*$^{c/-}$ (n=10), *Depdc5*$^{+/+}$ (n=7) and *Depdc5*$^{+/-}$ (n=3) mice to record brain activity by continuous video-EEG in free-moving animals. All ten *Depdc5*$^{c/-}$ mice died suddenly in a tonic posture; we were able to record six fatal seizures (the other four were not connected to the recording device at time of death) confirming spontaneous fatal electroclinical seizures. In 4/6 *Depdc5*$^{c/-}$ mice, a single seizure was immediately followed by sudden death (age at death: 83-116 days). In 2 out of 6

Depdc5$^{c/-}$ mice, recurrent spontaneous seizures occurred at a mean frequency of 1.14 seizure/day over a week before a terminal seizure (age at death: 106-117 days).

Attempting to define predictive biomarkers for SUDEP, we asked whether fatal and non-fatal seizures could be distinguished in term of age onset, seizure duration and behavior. The ages of occurrence of fatal and non-fatal seizures were similar (mean 103.5 ± 3.1 vs 102.5 ± 5.5 days, respectively) (Fig. 3D). The duration of fatal and non-fatal seizures was comparable (average 25 s, range 10-35 s, n=27 seizures; Fig. 3E). Fatal seizures occurred during both sleep and waking phases. The frequency of non-fatal seizures did not increase before the terminal seizure as reported in other mouse models of SUDEP[42,43]. EEG signal patterns were not strikingly different in non-fatal and fatal seizures: generalized high-amplitude spikes and polyspikes at 10-15 Hz, with no detectable focal onset. Fig. 3F-G show typical patterns and Fast Fourier Transform power spectra, which were similar for fatal and non-fatal seizures. Non-fatal seizures ended with a postictal generalized EEG suppression (PGES) of 4 min 30.6 ± 25.3 s before normal EEG activity was re-established, while for fatal seizures the PGES was prolonged indefinitely, coinciding with death of the animal. Duration of PGES associated with non-fatal seizures did not change over the days preceding the final SUDEP seizure and therefore could not predict the fatal seizure. Seizures consisted of a stereotyped sequence of behaviors: behavioral tonic arrest with short periods of forelimb clonus (Racine stage 3) was followed by rearing and falling to the side (Racine stage 4), a characteristic of a GTCS (videos shown in Supplementary Video 1-2, corresponding to non-fatal and fatal seizure respectively). While the duration of the tonic phase was similar between fatal and non-fatal seizures, duration of the clonic phase was shorter in fatal seizures, in which wild running was longer (Fig. 3H). Specifically, wild running (Racine stage 5) was observed in all fatal seizures, but only in 50% of non-fatal seizures, and episodes were shorter for non-fatal than for fatal seizures (duration 1.7 ± 0.7 vs 7.2 ± 1.4 s; Fig. 3I). Fatal seizures ended with hind limb extension. Control *Depdc5*$^{+/+}$ and heterozygous *Depdc5*$^{+/-}$ mice did not exhibit seizures or die prematurely.

In summary, all *Depdc5*$^{c/-}$ mice exhibited spontaneous GTCS. Fatal and non-fatal seizures had similar durations and frequencies and began at comparable ages. None of the parameters measured from EEG traces could be reliably linked with SUDEP-like events. Longer lasting wild running behaviors were more likely to precede sudden death. We next asked if alterations in cardiac activity could predispose *Depdc5*$^{c/-}$ mice to SUDEP and predict fatal seizures.

Cardiac investigation in *Depdc5*$^{c/-}$ mice

We first assessed baseline cardiac function in adult anesthetized mice (n=9 *Depdc5*$^{c/-}$ and n=9 *Depdc5*$^{+/+}$ mice). Representative ECG trace is shown in Fig. 4A. There were no significant differences in baseline heart rate, assessed with the RR length (144.5 ± 8.9 ms for *Depdc5*$^{c/-}$ vs. 141 ± 5.5 ms for *Depdc5*$^{+/+}$, p=0.75), PR length (46.9 ± 1.5 ms vs. 47.9 ± 2.1, p=0.7), QT interval (36.7 ± 1.4 ms vs. 33.4 ± 1.7, p=0.17) and QRS length (7.2 ± 0.3 ms vs. 6.8 ± 0.3, p=0.35) between *Depdc5*$^{c/-}$ and *Depdc5*$^{+/+}$ mice. To

complete the characterization of baseline cardiac function, we assessed the heart rate variability (HRV) with the SDRR parameter (0.054 ± 0.018 vs 0.039 ± 0.002, p>0.99), and the rMSSD parameter (0.62 ± 0.1 vs 0.42 ± 0.07, p=0.33), both indicating no significant differences between *Depdc5*$^{c/-}$ mice and controls.

Secondly, we performed simultaneous video EEG-ECG recordings to assess cardiac activity during fatal seizures in *Depdc5*$^{c/-}$ (n=23) compared to *Depdc5*$^{+/+}$ (n=4) conscious unrestrained mice. During the period preceding a seizure, the baseline heart rate was in the normal range (mean RR length = 95.33 ± 4.9 ms for *Depdc5*$^{c/-}$ vs. 94.7 ± 3.2 ms for *Depdc5*$^{+/+}$, p=0.57). The heart rate variability, assessed with SDRR (0.051 ± 0.009 vs 0.065 ± 0.005, p=0.46), rMSSD (1.52 ± 1.2 vs 1.77 ± 1.2, p=0.57), and with the short-term HRV (SD1) and long-term HRV (SD2) parameters of the Poincaré plots[38,39] showed no cardiac arrhythmia in *Depdc5*$^{c/-}$ mice (Fig. 4B).

In the ictal period, we were able to record SUDEP-events by simultaneous EEG-ECG signals in 6/23 *Depdc5*$^{c/-}$ mice at age of P98 ± 9. Representative EEG-ECG trace before, during and after a fatal seizure is shown in Fig. 4C. Electroclinical fatal seizures displayed a succession of tonic, clonic, wild-running phases, terminated by a tonic posturing with a hind limb extension (see Supplementary videos 2-3). During the tonic phase, cardiac activity assessed by RR intervals and heart rate was normal; a moderate heart rate increase (tachycardia) occurred during the clonic phase. During the wild-running phase, the RR intervals increased rapidly reflecting a variable and progressive slowing of the ventricular rate (Fig. 4C). After himb limb extension, during the PGES, the heart rate markedly decreased until cardiac arrest. Qualitative examination of videos show that a respiratory arrest occurred after the fatal seizure (see Supplementary videos 2-3). All six recorded fatal seizures presented the same pattern of EEG-ECG. On average, heart rate was normal (540 ± 20 bpm) before seizure and decreased to 250 ± 50 bpm at the end of the seizure (Fig. 4D), indicating that bradycardia followed by heart arrest 4 min later was consecutive of the fatal seizure, and not causal. We conclude that *Depdc5*$^{c/-}$ mice did not present primary cardiac abnormalities during the pre-ictal period of fatal seizures.

Finally, we investigated heart histology in *Depdc5*$^{c/-}$ mice, before and after SUDEP-like event. Compared to *Depdc5*$^{+/+}$ control (Fig. 5A), H&E stained transverse heart sections did not show structural differences before the seizure occurrence (Fig. 5B), nor after SUDEP-like events (Fig. 5C). Notably, no contraction band necrosis or fibrosis were observed in *Depdc5*$^{c/-}$ mice after SUDEP-like event (Fig. 5C).

Discussion

Mutations in either *DEPDC5*, *NPRL2*, or *NPRL3* are commonly encountered among subjects with childhood onset focal seizures either with a normal MRI or associated with a focal cortical dysplasia (FCD) type 2[17]. Several clinical observations suggest that mutations in *DEPDC5*, *NPRL2*, *NPRL3*, the components of the GATOR1 complex of the mTOR pathway, may confer a higher risk to SUDEP[15–18]. Mutations in GATOR1

genes cause a loss-of-function leading to a haploinsufficiency and hyperactivation of the mTOR signaling pathway[18,27,28,44]. Pathophysiological mechanisms that induce sudden death in GATOR1-related epilepsy remain unknown.

Epilepsy genes associated to SUDEP include cardiac and neuronal ion channel genes regulating excitability in both heart and brain, thus generating cardiac arrhythmias and seizures[8–11]. In this study, we asked whether DEPDC5-related SUDEP may have a primary cardiac etiology, and we aimed to identify possible predictive cardiac biomarkers. Whether DEPDC5 has a direct impact on cardiac activity and could lead to fatal seizures is a crucial question. This study shows that Depdc5 protein is expressed in the brain and the heart. Noteworthy, in a previous study[45], invalidation of Depdc5 in mouse skeletal muscle led to muscle cell hypertrophy and alterations of mitochondrial respiratory capacity, suggesting that Depdc5-deficiency could contribute to cardiac dysfunction.

For this purpose, we present here an unprecedented cohort of rare cases of 16 patients with *GATOR1* mutations that underwent cardiac evaluation because of risk for SUDEP, among which 6/16 at high-risk because of family history of SUDEP, and 3/16 who died of a SUDEP. There was no evidence for cardiac arrhythmia or structural abnormality on resting 12-lead ECG, Holter-ECG monitoring and TTE in any of the patients, suggesting that seizures did not have long-term inter-ictal consequences on cardiac activity. Notably, no clinical cardiac anomalies were detected in 3/3 patients carrying pathogenic *DEPDC5* variants who succumbed to SUDEP at 2, 3 and 7 years after cardiac assessment. All three SUDEP patients had received a sodium channel blocker antiseizure drug. While this treatment may increase the risk for sudden cardiac death[46], a recent large case-control study did not show any clear association between antiseizure medication and SUDEP, rather it showed an association between nonadherence and SUDEP[47]. Noticeably, SUDEP patient #16 had issues with medication compliance. The two other SUDEP patients (#1 & #2) had been seizure-free for at least 8 months before SUDEP, suggesting it is unlikely that a poor control of seizures could contribute to sudden cardiac death. We also present the first record of an autopsy on heart tissue in a *DEPDC5* patient, which revealed no structural pathology that might affect the integrity or electrical function of the heart. Myocardial fibrosis, previously reported at autopsy in some SUDEP cases[48], and contraction band necrosis, associated with sudden cardiac death[41], were absent. Altogether, our human data indicate that *DEPDC5*-related SUDEP is unlikely to result from primary fatal cardiac arrhythmia due to repetitive seizures or as a direct consequence of GATOR1 mutations on cardiac activity. This hitherto unique study suggests a distinct SUDEP mechanism between patients with *DEPDC5* mutations and patients with epilepsy ion channel gene mutations[10].

The clinical evaluation of patients has several limitations because of the lack of: 1) high resolution TTE capable of identifying subtle changes such as cardiac stiffness in people with epilepsy[49], although such stiffness is unlikely to have been present since fibrosis, a marker of cardiac stiffness[49], was not observed in the postmortem heart; 2) prolonged ECG recordings (only 4/16 patients had Holter-ECG monitoring, ranging

from 24 hours to 8 days); 3) ictal ECG recordings (only available in one patient during presurgical evaluation) which may reveal transient cardiac arrhythmias as previously reported[4]. In addition, the patient cohort size is relatively small, and we cannot completely exclude additional possibilities, such as dynamic alterations in cardiac electrophysiology, as seen in *ATP1A3*-related disease, another genetic disorder characterized by paroxysmal neurological events, including seizures[50].

The limits of both ante and post-mortem human clinical investigations prompted us to explore cardiac activity during seizures in a mouse model of SUDEP linked to *Depdc5* deficiency. Using a tagged HA-Depdc5 mouse, we show that Depdc5 protein is highly expressed in the cortex, in both excitatory and inhibitory neurons, but not in glial cells, in accord with mouse and human single-cell RNA-seq data[51]. As expected for an mTOR repressor[24], Depdc5 colocalized with lysosomes. During neurodevelopment, Depdc5 expression increased to a peak in adulthood, correlating with mTOR protein expression[52]. A recent report suggested that *Depdc5* knockdown in a mixed culture of excitatory and inhibitory cortical neurons enhances excitatory neurotransmission, with presumed pro-epileptic effects[53], which could be the cause of seizures related to *DEPDC5* deficiency.

We next generated a mouse model with a *Depdc5* neuronal deletion in Synapsin1-cre expressing neurons on a *Depdc5* heterozygous background to mimic brain second-hit events reported in patients with FCD type 2[18–22,30]. All *Depdc5*$^{c/-}$ mice exhibited spontaneous seizures with a fatal outcome at ~3 months of age. While few *Depdc5*$^{c/-}$ mice presented non-fatal seizures preceding the fatal one, most of them had a single seizure that proved fatal. This notable observation has its parallel in the histories of two patients (#1 and #2) who had been seizure-free for prolonged intervals (9 years and 8 months, respectively) before succumbing to SUDEP. The established clinical feature most strongly associated with SUDEP risk is the uncontrolled tonic-clonic seizures[3,4]. Neither of these patients were reported to have such seizures, and both died after prolonged periods of seizure freedom, raising questions about our current ideas on the mechanisms of SUDEP.

Cardiac activity of *Depdc5*$^{c/-}$ mice showed no significant alterations, nor different HRV compared to controls, which could have predicted or predisposed to a fatal seizure. HRV, a marker of autonomic tone[39,54], was not impaired suggesting autonomic function is not altered. ECG recordings during fatal seizures revealed a short tachycardia, followed by a progressive bradycardia, which are cardiac features that can be associated with typical epileptic seizures[55]. Therefore, no obvious cardiological defects were present in the *Depdc5*$^{c/-}$ mice, nor autonomic dysfunction that could impact arrhythmogenesis, as mentioned in sudden cardiac death[56].

Cerebral biomarkers of SUDEP are still missing, and so far, GTCS represent the greatest risk factor for SUDEP in humans[4,5,7,57]. Comparison of fatal and non-fatal seizures in *Depdc5*$^{c/-}$ mice showed fatal seizures were accompanied by a longer episode of wild running while GTCS electrographic features were similar. This wild running behavior is reported during audiogenic seizures, where the brainstem may be

involved[58]. Brainstem nuclei control visceral functions including cardiac and respiratory pacemakers. Brainstem dysfunction has been linked to SUDEP where postictal apnea and bradycardia precede asystole and death[5]. Spreading depolarization in the brainstem mediates sudden cardiorespiratory arrest in both genetic and induced mouse SUDEP models[39,59]. Our data suggest that SUDEP-like event due to Depdc5 haploinsufficiency might be a consequence of brainstem failure, rather than a predisposition to cardiac arrhythmia.

In conclusion, we report a non-ion channel SUDEP mouse model, and our data do not support primary cardiac etiology as the proximate cause of death. Canonical cardiac biomarkers such as QT interval or heart rate are poor predictors of sudden death in *DEPDC5*-mutated patients, in contrast to SUDEP cases linked to ion-channel gene mutations[10]. Effective preventive strategies in high-risk patients will rely on the understanding of the mechanisms that lead from seizures to death.

Acknowledgements

We thank the families that took part in this study, Dr Joel Devendeville for sharing the autopsy material, Dr Richard Miles for proofreading the article and the clinicians who performed cardiac exams. We also thank the ICM core facilities: PHENO-ICMice, ICM.Quant, Histomics, iGenSeq, CELIS, DNA and cell bank. All animal work was conducted at the PHENO-ICMice facility (supported by ANR-10- IAIHU-06 and ANR-11-INBS-0011-NeurATRIS and FRM). This research was made possible through access to the data and findings generated by the 100,000 Genomes Project. The 100,000 Genomes Project is managed by Genomics England Limited (a wholly owned company of the Department of Health and Social Care). The 100,000 Genomes Project uses data provided by patients and collected by the National Health Service as part of their care and support. This work was funded by the European Research Council (N°682345 to SB), the program "Investissements d'avenir" (ANR-10-IAIHU-06) and the Fondation pour la Recherche Médicale, (FDT201904008269 to TR). Part of this work was undertaken at University College London Hospitals, which received a proportion of funding from the NIHR Biomedical Research Centres funding scheme. Additional funding was provided by the Epilepsy Society. The 100,000 Genomes Project is funded by the National Institute for Health Research and NHS England. The Wellcome Trust, Cancer Research UK and the Medical Research Council have also funded research infrastructure.

Author Contributions

AB and SB contributed to the conception and design of the study; AB, DR, TB, SZ, MM, TR, HAB, CM, MJ, IA, and FP contributed to the acquisition and analysis of data; AB, DR, TB, VN, SMS and SB contributed to drafting the text and preparing the figures.

Potential Conflicts of Interest

The authors have declared no conflict of interest.

References

1. Nashef L, So EL, Ryvlin P, Tomson T. Unifying the definitions of sudden unexpected death in epilepsy. *Epilepsia*. 2012;53(2):227-233. doi:10.1111/j.1528-1167.2011.03358.x

2. Harden C, Tomson T, Gloss D, et al. Practice Guideline Summary: Sudden Unexpected Death in Epilepsy Incidence Rates and Risk Factors: Report of the Guideline Development, Dissemination, and Implementation Subcommittee of the American Academy of Neurology and the American Epilepsy Society. *Epilepsy Curr*. 2017;17(3):180-187. doi:10.5698/1535-7511.17.3.180

3. Whitney R, Donner EJ. Risk Factors for Sudden Unexpected Death in Epilepsy (SUDEP) and Their Mitigation. *Curr Treat Options Neurol*. 2019;21(2):7. doi:10.1007/s11940-019-0547-4

4. Ryvlin P, Nashef L, Lhatoo SD, et al. Incidence and mechanisms of cardiorespiratory arrests in epilepsy monitoring units (MORTEMUS): a retrospective study. *Lancet Neurol*. 2013;12(10):966-977. doi:10.1016/S1474-4422(13)70214-X

5. Devinsky O, Hesdorffer DC, Thurman DJ, Lhatoo S, Richerson G. Sudden unexpected death in epilepsy: epidemiology, mechanisms, and prevention. *Lancet Neurol*. 2016;15(10):1075-1088. doi:10.1016/S1474-4422(16)30158-2

6. Lacuey N, Zonjy B, Hampson JP, et al. The incidence and significance of periictal apnea in epileptic seizures. *Epilepsia*. 2018;59(3):573-582. doi:10.1111/epi.14006

7. Pensel MC, Nass RD, Taubøll E, Aurlien D, Surges R. Prevention of sudden unexpected death in epilepsy: current status and future perspectives. *Expert Rev Neurother*. 2020;20(5):497-508. doi:10.1080/14737175.2020.1754195

8. Friedman D, Kannan K, Faustin A, et al. Cardiac arrhythmia and neuroexcitability gene variants in resected brain tissue from patients with sudden unexpected death in epilepsy (SUDEP). *NPJ genomic medicine*. 2018;3:9. doi:10.1038/s41525-018-0048-5

9. Chahal CAA, Salloum MN, Alahdab F, et al. Systematic Review of the Genetics of Sudden Unexpected Death in Epilepsy: Potential Overlap With Sudden Cardiac Death and Arrhythmia-Related Genes. *J Am Heart Assoc*. 2020;9(1):e012264. doi:10.1161/JAHA.119.012264

10. Bleakley LE, Soh MS, Bagnall RD, et al. Are Variants Causing Cardiac Arrhythmia Risk Factors in Sudden Unexpected Death in Epilepsy? *Front Neurol*. 2020;11:925. doi:10.3389/fneur.2020.00925

11. Bagnall RD, Crompton DE, Semsarian C. Genetic Basis of Sudden Unexpected Death in Epilepsy. *Front Neurol*. 2017;8:348. doi:10.3389/fneur.2017.00348

12. Zijlmans M, Flanagan D, Gotman J. Heart Rate Changes and ECG Abnormalities During Epileptic Seizures: Prevalence and Definition of an Objective Clinical Sign. *Epilepsia*. 2002;43(8):847-854. doi:https://doi.org/10.1046/j.1528-1157.2002.37801.x

13. Massey CA, Sowers LP, Dlouhy BJ, Richerson GB. Mechanisms of sudden unexpected death in epilepsy: the pathway to prevention. *Nat Rev Neurol*. 2014;10(5):271-282. doi:10.1038/nrneurol.2014.64

14. Schwartz PJ, Ackerman MJ, George AL, Wilde AAM. Impact of genetics on the clinical management of channelopathies. *J Am Coll Cardiol*. 2013;62(3):169-180. doi:10.1016/j.jacc.2013.04.044

15. Nascimento FA, Borlot F, Cossette P, Minassian BA, Andrade DM. Two definite cases of sudden unexpected death in epilepsy in a family with a DEPDC5 mutation. *Neurol Genet*. 2015;1(4):e28. doi:10.1212/NXG.0000000000000028

16. Bagnall RD, Crompton DE, Petrovski S, et al. Exome-based analysis of cardiac arrhythmia, respiratory control, and epilepsy genes in sudden unexpected death in epilepsy. *Ann Neurol*. 2016;79(4):522-534. doi:10.1002/ana.24596

17. Baldassari S, Picard F, Verbeek NE, et al. The landscape of epilepsy-related GATOR1 variants. *Genet Med*. 2019;21(2):398-408. doi:10.1038/s41436-018-0060-2

18. Weckhuysen S, Marsan E, Lambrecq V, et al. Involvement of GATOR complex genes in familial focal epilepsies and focal cortical dysplasia. *Epilepsia*. 2016;57(6):994-1003. doi:10.1111/epi.13391

19. Ribierre T, Deleuze C, Bacq A, et al. Second-hit mosaic mutation in mTORC1 repressor DEPDC5 causes focal cortical dysplasia-associated epilepsy. *J Clin Invest*. 2018;128(6):2452-2458. doi:10.1172/JCI99384

20. Yuskaitis CJ, Jones BM, Wolfson RL, et al. A mouse model of DEPDC5-related epilepsy: Neuronal loss of Depdc5 causes dysplastic and ectopic neurons, increased mTOR signaling, and seizure susceptibility. *Neurobiol Dis*. 2018;111:91-101. doi:10.1016/j.nbd.2017.12.010

21. Yuskaitis CJ, Rossitto L-A, Gurnani S, Bainbridge E, Poduri A, Sahin M. Chronic mTORC1 inhibition rescues behavioral and biochemical deficits resulting from neuronal Depdc5 loss in mice. *Hum Mol Genet*. 2019;28(17):2952-2964. doi:10.1093/hmg/ddz123

22. Klofas LK, Short BP, Zhou C, Carson RP. Prevention of premature death and seizures in a Depdc5 mouse epilepsy model through inhibition of mTORC1. *Hum Mol Genet*. 2020;29(8):1365-1377. doi:10.1093/hmg/ddaa068

23. Bar-Peled L, Chantranupong L, Cherniack AD, et al. A Tumor suppressor complex with GAP activity for the Rag GTPases that signal amino acid sufficiency to mTORC1. *Science*. 2013;340(6136):1100-1106. doi:10.1126/science.1232044

24. Shen K, Huang RK, Brignole EJ, et al. Architecture of the human GATOR1 and GATOR1-Rag GTPases complexes. *Nature*. 2018;556(7699):64-69. doi:10.1038/nature26158

25. Liu GY, Sabatini DM. mTOR at the nexus of nutrition, growth, ageing and disease. *Nat Rev Mol Cell Biol*. 2020;21(4):183-203. doi:10.1038/s41580-019-0199-y

26. Dibbens LM, de Vries B, Donatello S, et al. Mutations in DEPDC5 cause familial focal epilepsy with variable foci. *Nat Genet*. 2013;45(5):546-551. doi:10.1038/ng.2599

27. Ishida S, Picard F, Rudolf G, et al. Mutations of DEPDC5 cause autosomal dominant focal epilepsies. *Nat Genet*. 2013;45(5):552-555. doi:10.1038/ng.2601

28. Picard F, Makrythanasis P, Navarro V, et al. DEPDC5 mutations in families presenting as autosomal dominant nocturnal frontal lobe epilepsy. *Neurology*. 2014;82(23):2101-2106. doi:10.1212/WNL.0000000000000488

29. Ricos MG, Hodgson BL, Pippucci T, et al. Mutations in the mammalian target of rapamycin pathway regulators NPRL2 and NPRL3 cause focal epilepsy. *Ann Neurol*. 2016;79(1):120-131. doi:10.1002/ana.24547

30. Baldassari S, Ribierre T, Marsan E, et al. Dissecting the genetic basis of focal cortical dysplasia: a large cohort study. *Acta Neuropathol*. 2019;138(6):885-900. doi:10.1007/s00401-019-02061-5

31. Baulac S, Ishida S, Marsan E, et al. Familial focal epilepsy with focal cortical dysplasia due to DEPDC5 mutations. *Ann Neurol*. 2015;77(4):675-683. doi:10.1002/ana.24368

32. Lee WS, Stephenson SEM, Howell KB, et al. Second-hit DEPDC5 mutation is limited to dysmorphic neurons in cortical dysplasia type IIA. *Ann Clin Transl Neurol*. 2019;6(7):1338-1344. doi:10.1002/acn3.50815

33. Sim NS, Ko A, Kim WK, et al. Precise detection of low-level somatic mutation in resected epilepsy brain tissue. *Acta Neuropathol*. 2019;138(6):901-912. doi:10.1007/s00401-019-02052-6

34. Basso C, Aguilera B, Banner J, et al. Guidelines for autopsy investigation of sudden cardiac death: 2017 update from the Association for European Cardiovascular Pathology. *Virchows Archiv: An International Journal of Pathology*. 2017;471(6):691-705. doi:10.1007/s00428-017-2221-0

35. Marsan E, Ishida S, Schramm A, et al. Depdc5 knockout rat: A novel model of mTORopathy. *Neurobiol Dis*. 2016;89:180-189. doi:10.1016/j.nbd.2016.02.010

36. Franklin K, Paxinos G. *The Mouse Brain in Stereotaxic Coordinates, Compact - 3rd Edition*. Academic Press.; 2008. Accessed December 8, 2020. https://www.elsevier.com/books/the-mouse-brain-in-stereotaxic-coordinates-compact/franklin/978-0-12-374244-5

37. Mishra V, Gautier NM, Glasscock E. Simultaneous Video-EEG-ECG Monitoring to Identify Neurocardiac Dysfunction in Mouse Models of Epilepsy. *J Vis Exp*. 2018;(131):57300. doi:10.3791/57300

38. Kamen PW, Krum H, Tonkin AM. Poincaré Plot of Heart Rate Variability Allows Quantitative Display of Parasympathetic Nervous Activity in Humans. *Clinical Science*. 1996;91(2):201-208. doi:10.1042/cs0910201

39. Kim Y, Bravo E, Thirnbeck CK, et al. Severe peri-ictal respiratory dysfunction is common in Dravet syndrome. *J Clin Invest*. 2018;128(3):1141-1153. doi:10.1172/JCI94999

40. Charan J, Kantharia ND. How to calculate sample size in animal studies? *J Pharmacol Pharmacother*. 2013;4(4):303-306. doi:10.4103/0976-500X.119726

41. Hopster DJ, Milroy CM, Burns J, Roberts NB. Necropsy study of the association between sudden cardiac death, cardiac isoenzymes and contraction band necrosis. *Journal of Clinical Pathology*. 1996;49(5):403-406. doi:10.1136/jcp.49.5.403

42. Ren Y, Chang J, Li C, et al. The Effects of Ketogenic Diet Treatment in Kcna1-Null Mouse, a Model of Sudden Unexpected Death in Epilepsy. *Front Neurol*. 2019;10:744. doi:10.3389/fneur.2019.00744

43. Teran FA, Kim Y, Crotts MS, Bravo E, Emaus KJ, Richerson GB. Time of Day and a Ketogenic Diet Influence Susceptibility to SUDEP in Scn1aR1407X/+ Mice. *Front Neurol*. 2019;10:278. doi:10.3389/fneur.2019.00278

44. Sim JC, Scerri T, Fanjul-Fernández M, et al. Familial cortical dysplasia caused by mutation in the mammalian target of rapamycin regulator NPRL3. *Ann Neurol*. 2016;79(1):132-137. doi:10.1002/ana.24502

45. Graber TG, Fry CS, Brightwell CR, et al. Skeletal muscle-specific knockout of DEP domain containing 5 protein increases mTORC1 signaling, muscle cell hypertrophy, and mitochondrial respiration. *J Biol Chem*. 2019;294(11):4091-4102. doi:10.1074/jbc.RA118.005970

46. Bardai A, Blom MT, van Noord C, Verhamme KM, Sturkenboom MCJM, Tan HL. Sudden cardiac death is associated both with epilepsy and with use of antiepileptic medications. *Heart*. 2015;101(1):17-22. doi:10.1136/heartjnl-2014-305664

47. Sveinsson O, Andersson T, Mattsson P, Carlsson S, Tomson T. Pharmacologic treatment and SUDEP risk: A nationwide, population-based, case-control study. *Neurology*. 2020;95(18):e2509-e2518. doi:10.1212/WNL.0000000000010874

48. P-Codrea Tigaran S, Dalager-Pedersen S, Baandrup U, Dam M, Vesterby-Charles A. Sudden unexpected death in epilepsy: is death by seizures a cardiac disease? *Am J Forensic Med Pathol*. 2005;26(2):99-105.

49. Fialho GL, Pagani AG, Wolf P, Walz R, Lin K. Echocardiographic risk markers of sudden death in patients with temporal lobe epilepsy. *Epilepsy Res*. 2018;140:192-197. doi:10.1016/j.eplepsyres.2018.01.016

50. Balestrini S, Mikati MA, Álvarez-García-Rovés R, et al. Cardiac phenotype in ATP1A3-related syndromes: A multicenter cohort study. *Neurology*. 2020;95(21):e2866-e2879. doi:10.1212/WNL.0000000000010794

51. Hodge RD, Bakken TE, Miller JA, et al. Conserved cell types with divergent features in human versus mouse cortex. *Nature*. 2019;573(7772):61-68. doi:10.1038/s41586-019-1506-7

52. Talos DM, Sun H, Zhou X, et al. The Interaction between Early Life Epilepsy and Autistic-Like Behavioral Consequences: A Role for the Mammalian Target of Rapamycin (mTOR) Pathway. *PLOS ONE*. 2012;7(5):e35885. doi:10.1371/journal.pone.0035885

53. De Fusco A, Cerullo MS, Marte A, et al. Acute knockdown of Depdc5 leads to synaptic defects in mTOR-related epileptogenesis. *Neurobiol Dis*. 2020;139:104822. doi:10.1016/j.nbd.2020.104822

54. Verrier RL, Pang TD, Nearing BD, Schachter SC. Epileptic heart: A clinical syndromic approach. *Epilepsia*. 2021;62(8):1780-1789. doi:10.1111/epi.16966

55. Jefferys JGR, Ashby-Lumsden A, Lovick TA. Cardiac effects of repeated focal seizures in rats induced by intrahippocampal tetanus toxin: Bradyarrhythmias, tachycardias, and prolonged interictal QT interval. *Epilepsia*. 2020;61(4):798-809. doi:10.1111/epi.16479

56. Verrier RL, Pang TD, Nearing BD, Schachter SC. Epileptic heart: A clinical syndromic approach. *Epilepsia*. n/a(n/a). doi:10.1111/epi.16966

57. King-Stephens D. Biomarkers for SUDEP: Are We There Yet? *Epilepsy Curr*. 2019;19(4):231-233. doi:10.1177/1535759719855948

58. Faingold CL. Brainstem Networks: Reticulo-Cortical Synchronization in Generalized Convulsive Seizures. In: Noebels JL, Avoli M, Rogawski MA, Olsen RW, Delgado-Escueta AV, eds. *Jasper's Basic Mechanisms of the Epilepsies*. 4th ed. National Center for Biotechnology Information (US); 2012. Accessed December 14, 2020. http://www.ncbi.nlm.nih.gov/books/NBK98187/

59. Aiba I, Noebels JL. Spreading depolarization in the brainstem mediates sudden cardiorespiratory arrest in mouse SUDEP models. *Sci Transl Med*. 2015;7(282):282ra46. doi:10.1126/scitranslmed.aaa4050

Table 1. Genetic features and SUDEP history of the patient cohort

Case	Gender	Gene: variant	SUDEP	Family history of SUDEP	Ref
1	F	*DEPDC5*: p.Arg874*	Definite SUDEP during night at 18y	Paternal granduncle died of probable SUDEP at 59y after a diurnal sz	18
2	F	*DEPDC5*: p.Glu1385*	Probable SUDEP during night at 50y	No	18
3	M	*DEPDC5*: p.Glu1421Argfs*	No	No	17
4	M	*DEPDC5*: p.Met152fs	No	No	17
5	F	*NPRL2*: p.Ile23Asnfs*6	No	Uncle died of probable SUDEP at 22y	17
6	F	*NPRL3*: p.Arg424*	No	Half-sister died of probable SUDEP at 25y, and two cousins had near-SUDEP at 30y	17
7	M	*DEPDC5:* p.Arg243*	No	No	
8	F	*DEPDC5:* p.Tyr1082*	No	Father died of probable SUDEP	
9	F	*DEPDC5:* p.Gln981*	No	No	
10	F	*DEPDC5:* p.Arg422*	No	No	
11	F	*DEPDC5:* p.Arg264GlufsTer9	No	Father died of possible SUDEP at 40y	
12	M	*DEPDC5:* c.3564-3C>G	No	No	
13	F	*DEPDC5:* p.E448*	No	Brother died of definite SUDEP at 21y	
14	M	*DEPDC5:* p.R1087*	No	No	
15	M	*DEPDC5*:c.280-1G>A	No	No	
16	M	*DEPDC5:* c.523_526del:p.I175Rfs*2	Probable SUDEP during night at 20y	No	

DEPDC5 (Refseq NM_001242896; NP_001229825), *NPRL2* (Refseq NM_006545; NP_006536) and *NPRL3* (Refseq NM_001077350; NP_001070818). Sz: seizure, y: years.

Table 2. Epilepsy features of the patient cohort

Case	Epilepsy type; age at onset	Seizure frequency	Antiseizure medication; outcome	Sodium channel blocker	Brain MRI	EEG/sEEG
1	SHE; 7y	NA	Low dosage of CBZ (recurrence after withdrawal); good outcome	Yes	Negative (1.5T)	Interictal EEG: normal
2	SHE; 12y	4-10 sz/year	TPM + LTG, CBZ added at 44, sz free for 8m before SUDEP	Yes	Negative	EEG: bifrontal epileptic activity
3	SHE; 5y	Several sz/night several days per week	CBZ, LVT	Yes	Negative (1.5T)	Interictal EEG: normal, sEEG: right insula onset
4	SHE; 4y	One nocturnal convulsive sz/month	CLB, OXC, PER; drug-resistant	Yes	Negative	Ictal EEG: right fronto-central seizure
5	FLE (operated at 18y: FCD 1); 3y	One nocturnal convulsive sz/month	LAC, CLB; drug-resistant	Yes	Negative (1.5T)	sEEG: right fronto basal and insular onset
6	FLE; 8y	Monthly to weekly nocturnal focal frontal sz	OXC, LTG, VPA, PER; drug-resistant	Yes	Negative (1.5T)	EEG: frontal epileptic activity
7	FLE (left frontal lobectomy, sz recurrence afterwards); 11y	Two clusters of two focal to bilateral tonic-clonic sz/month	VPA, LTG, PHE, rescue protocol with midazolam after the first sz; drug-resistant	Yes	Negative (3T)	EEG: left frontal lobe epilepsy. sEEG: left orbitofrontal lobe epilepsy
8	Focal epilepsy, localization unclear, 7y	2-4 focal to bilateral tonic-clonic sz/month, almost all arising from sleep	LTG, TPM	Yes	Negative (3T)	EEG (3 days VT): focal epilepsy, localization unclear (most likely left fronto-temporal)
9	Focal epilepsy, left neocortical temporal onset; 4y	1-2 focal sz with or without impaired awareness every two weeks, rare focal to bilateral tonic-clonic sz	LEV, VPA, clobazam	No	Negative (3T)	EEG (VT): neocortical focal epilepsy, possible left lateral temporal region
10	FTE, lateralization unclear; 1y	Brief blank spells 2-3 times per week. No focal to bilateral tonic-clonic sz	VPA, LAC	Yes	Negative (3T)	EEG (VT): interictal epileptiform discharges from both temporal regions
11	FTE; 7y	No clear sz, but frequent syncopal episodes (most likely of autonomic origin)	LTG	Yes	Mild cerebellar atrophy, small right parafal-cine menin-gioma (3T)	EEG: bitemporal interictal epileptiform activity, more prominent on the left
12	Focal epilepsy, left parietal onset; surgically resected FCD type 2; 7y	Sz free after lesionectomy	LAC, PER, TPM, clobazam	Yes	Left parietal FCD (3T)	Presurgical VT: Ictal bradycardia down to 42bpm
13	Focal epilepsy, left hemispheric onset; 11y	3-7 sz/week (30-40%: focal to bilateral tonic-clonic sz and others: focal impaired awareness sz)	OXC, TPM, rescue protocol with lorazepam and CLB	Yes	Negative (3T)	VT: focal epilepsy, left hemispheric onset, localization unclear
14	Focal epilepsy; 10y	Sz free for 3 years	LEV, LTG, CBZ	Yes	Negative (3T)	24h ambulatory EEG (23y), normal
15	FTE, 27y	Sz free for the past two years	BRV, ZNS, Pregabalin	No	Negative (3T)	24h ambulatory EEG: left temporal slow, no clear interictal

						epileptiform abnormalities.
16	Focal epilepsy; 7y	One unprovoked nocturnal convulsive sz every 2-3 months (but issues with medication compliance)	OXC	Yes	Negative	24h ambulatory EEG: bihemispheric cortical dysfunction, suggestive of multifocal irritative regions

Cases written in bold are the ones who succumbed from SUDEP. FLE: Frontal Lobe epilepsy, FTE: Focal temporal epilepsy, Sz: seizure; SHE: Sleep-related hypermotor sz; sEEG: stereotaxic EEG; VT: Video Telemetry; y: years.
Antiseizure medication: BRV: brivaracetam, CBZ: carbamazepine, CLB: clonazepam, LAC: lacosamide, LTG: lamotrigine, LEV: levetiracetam, OXC: oxcarbazepine, PER: perampanel, PB: phenobarbitone, PHE: phenytoin, PGB: pregabalin, TPM: topiramate, VPA: valproate, ZNS: zonisamide.

Table 3. Clinical cardiac features of the patient cohort

Case	Age at cardiac exam	12-lead ECG	Holter	Transthoracic echocardiogram (TTE)
1	16y	Normal (HR 68bpm, PR < 200ms, QRS < 120ms, QTc < 460ms)	NA	Normal
2	43y	Normal (HR 75bpm, PR 160ms, QRS 60ms, QTc 390ms)	NA	NA
3	36y	Normal including an optimal cardiac stress test (HR 75bpm, PR 114ms, QRS 78ms, QTc 389ms)	Normal (24h monitoring with rare SVES)	Normal
4	32y	Normal (HR 79bpm, PR 140ms, QRS <80ms, QTc <440ms)	Normal (24h monitoring with rare SVES)	Normal
5	29y	Normal (HR 80bpm, PR 180ms, QRS 60ms, QTc 362ms)	Normal (24h monitoring with rare SVES and one VES)	Normal (isolated subtle type I mitral regurgitation)
6	47y	Subnormal; isolated incomplete right bundle branch block (HR 62bpm, PR 180ms, QRS 100ms, QTc 360ms)	Normal (8-day monitoring with rare VES)	Normal (isolated ventricular septal aneurysm)
7	28y	Normal (HR 78bpm, PR 144ms, QRS 106ms, QTc 424ms)	NA	NA
8	47y	Normal (HR 61bpm, PR 142ms, QRS 80ms, QTc 422ms)	NA	NA
9	51y, 60y	51y: normal (HR 60bpm) 60y: Junctional rhythm (HR 52bpm, QRS 86ms, QTc 407ms)	NA	NA
10	41y	Normal with incomplete right bundle branch block (HR 66bpm, PR 164ms, QRS 100ms, QTc 448ms)	NA	NA
11	59y	Normal (HR 71bpm, PR 152ms, QRS 76ms, QTc 434ms). 24h monitoring: HR 80bpm Positive tilt testing: mild sympathetic failure and orthostatic intolerance	NA	NA
12	46y	Normal (HR 70bpm, borderline left axis deviation, PR 170ms, borderline T wave abnormalities, QTc 413ms)	NA	NA
13	35y, 45y	35y: Normal (HR 68bpm, PR 176ms, QRS 88ms)	Normal	45y: Normal
14	23y	Normal (HR 64bpm, PR 140ms, QRS 90ms, QTc 418ms)	NA	NA
15	50y	Normal (HR 70bpm, PR 154ms, QRS 86ms, QTc 403ms). Cardiac Computed Tomography: angiogram for chest pain, normal	NA	NA
16	18y	Normal (HR 50bpm, PR 136ms, QRS < 120ms, QTc < 450ms)	NA	NA

Cases written in bold are the ones who succumbed from SUDEP. HR: heart rate; SVES: supra ventricular extra systole; TTE: Transthoracic echocardiography; VES: ventricular extra systole; y: years. NA: Not assessed.

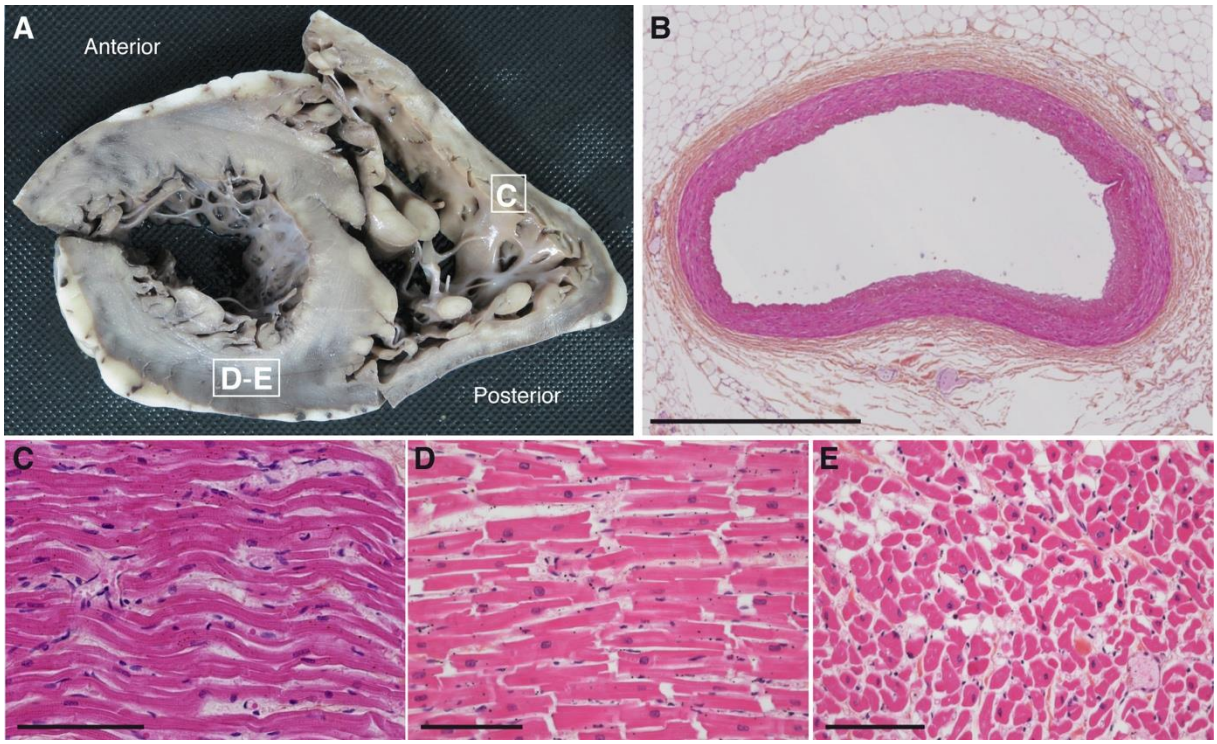

Figure 1. Macroscopic and microscopic pictures of the heart autopsy of patient #1. (**A**) Short axis view of a transverse section of the right and left ventricles. Morphological cardiovascular examination including valves and coronary arteries inspection revealed no gross abnormalities. White squares indicate sites of sections used for histological analysis in C-E. (**B**-**D**) Hematoxylin and eosin (H&E) stained transversal sections of the anterior interventricular artery (**B**), longitudinal sections of the right ventricle myocardium (**C**), the posterior wall of the left ventricle myocardium (**D**) and cross-sectional section of the left ventricle (**E**). No contraction band necrosis was detected. Scale bars represent 1 mm (**B**),100 µm (**C**-**E**).

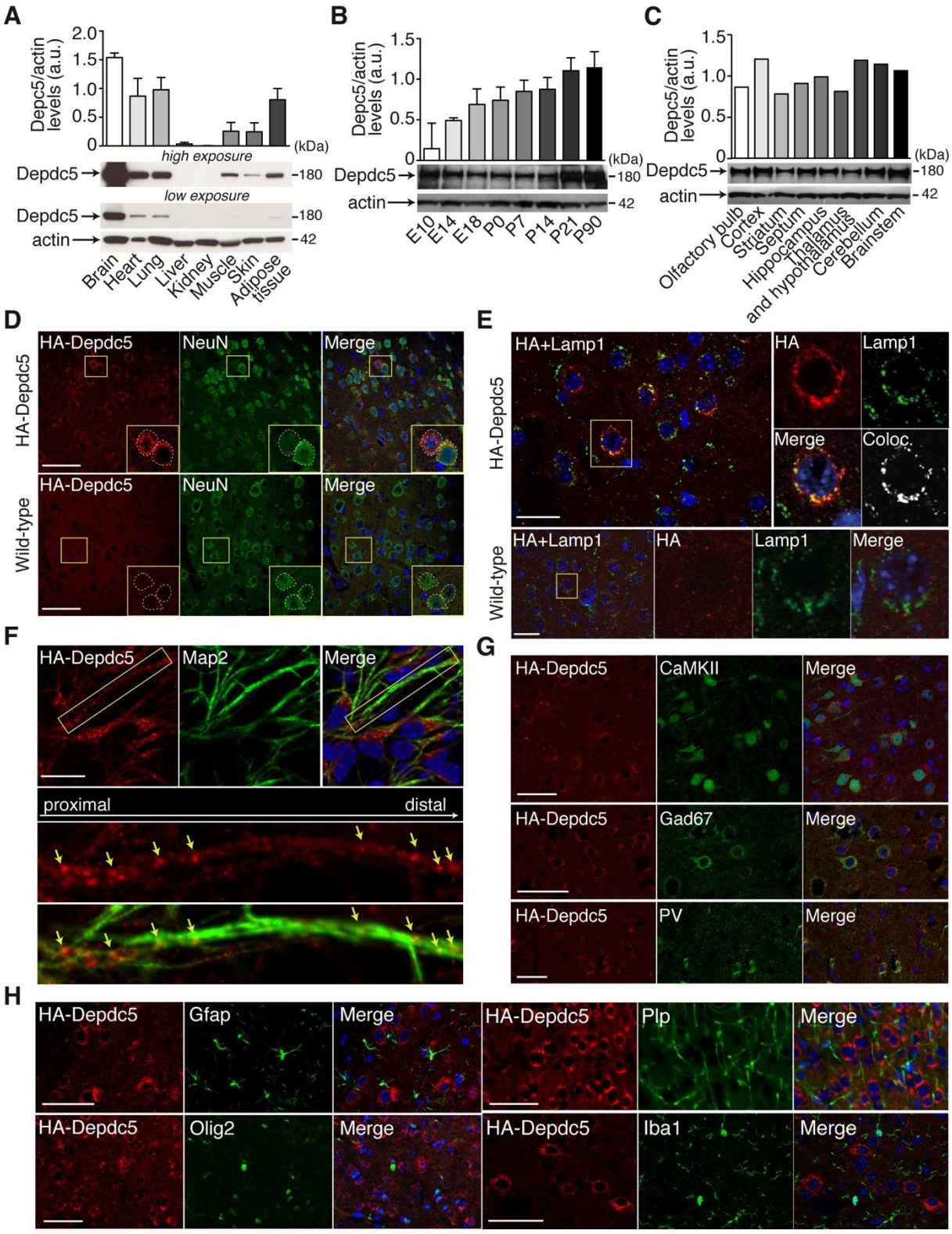

Figure 2. Depdc5 expression in the HA-tagged Depdc5 mouse. (**A**-**C**) Quantified representative Western blots show HA-Dedpc5 expression in (**A**) various mouse organ lysates, (**B**) mouse brain lysates at developmental stages from embryonic day 10 (E10) to postnatal day 90 (P90), and (**C**) in different brain regions of adult mouse (n=1-3). Actin was used as the loading control. (**D**-**H**) Depdc5 expression in the somatosensory cortex. (**D**) Immunofluorescent co-labeling of HA-Depdc5 (red) with NeuN (green)

showing specific expression of Depdc5 (compared to wild-type untagged cortex, bottom) in neuronal soma (see insets, corresponding to the yellow squares). (**E**) Immunofluorescent co-labeling of HA-Depdc5 (red) with Lamp1 (green) showing specific enriched expression in lysosomes (compared to wild-type untagged cortex, bottom). On right of insets (corresponding to the yellow square) are the colocalization between HA and Lamp1 (Pearson's correlation coefficient for HA-Depdc5 mouse = 0.49). (**F**) Immunofluorescent co-labeling of HA-Depdc5 (red) with Map2 (green) showing expression of Depdc5 in neuronal neurites. Bottom images are the insets (corresponding to yellow square) showing HA (red) distribution along the MAP2-positive (green) neurite. Arrows show aggregation of HA-Depdc5 staining. (**G**) Immunofluorescent co-labeling of HA-Depdc5 (red) and CaMKII (excitatory neurons), Gad67 (inhibitory neurons) or PV (Parvalbumin interneurons) shows Depdc5 is expressed in excitatory and inhibitory neurons. (**H**) Co-labeling of HA-Depdc5 (red) and Gfap, Olig2, Plp and Iba1, shows no co-expression in glial and microglial cells. N=3 sections done in duplicate. Scale bars represent 50 µm (**D**, **G-H**), 25 µm (**E**) and 20 µm (**F**).

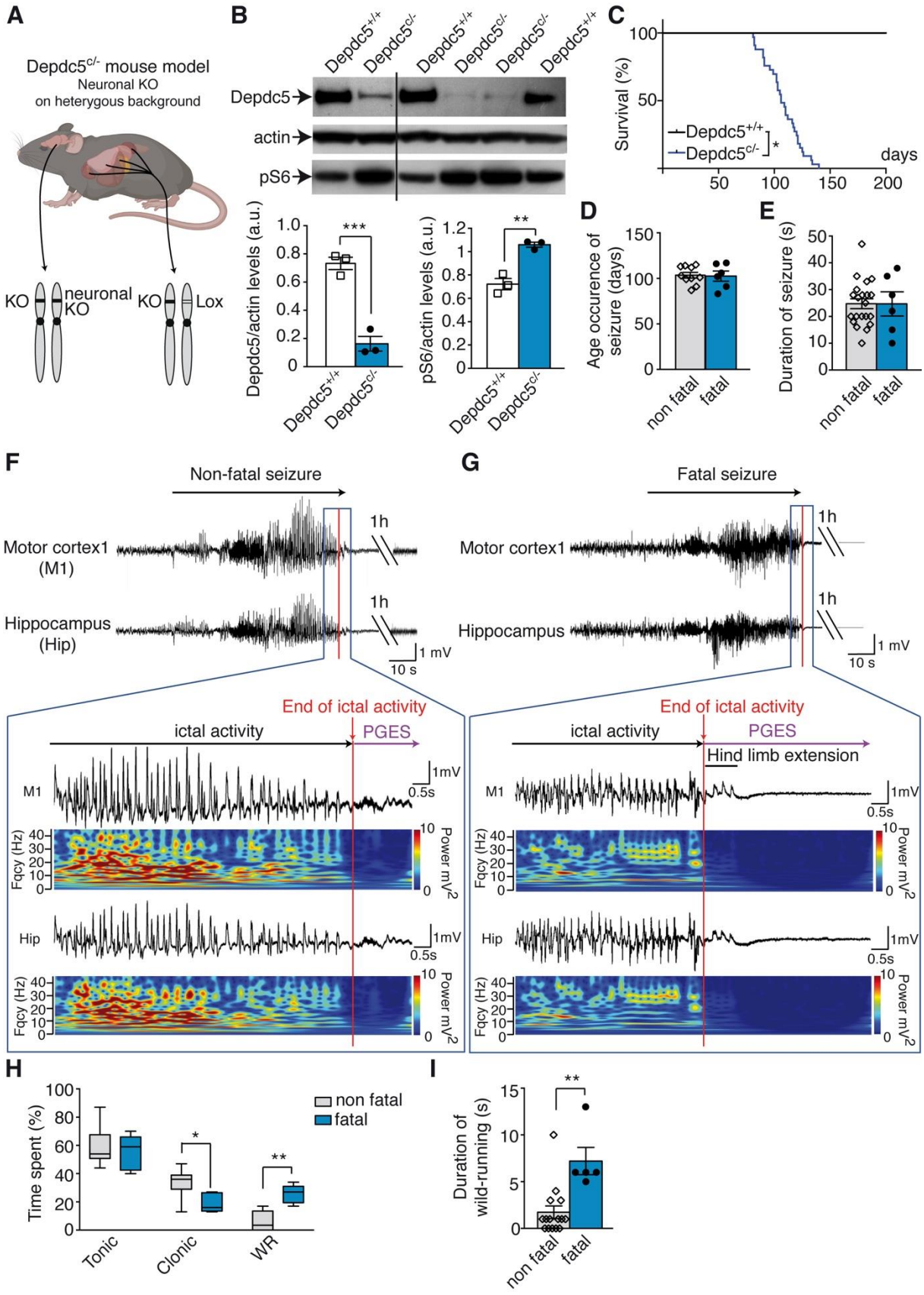

Figure 3. Spontaneous seizures in Depdc5$^{c/-}$ mice. (**A**) Illustration of the *Depdc5*$^{c/-}$ mouse model generated (KO = Knock-out). (**B**) Representative Western blot of brain lysates from *Depdc5*$^{c/-}$ and control wild-type (Depdc5$^{+/+}$) immunostained for Depdc5,

actin and pS6 (top) and quantification (bottom) of Depdc5 levels (left, unpaired t-test, $t_4 = 8.4$, $p = 0.0006$) and pS6 levels (right, unpaired t-test, $t_4 = 6.4$, $p = 0.0031$). (**C**) Survival of *Depdc5*$^{c/-}$ mice (n=33, log-rank test, $p = 0.047$). (**D**) Age at onset of non-fatal (n=6) and fatal seizures (n=10, unpaired t-test, $t_{14} = 0.17$, $p = 0.87$). (**E**) Duration of non-fatal (n=6) and fatal seizures (n=21, unpaired t-test, $t_{25} = 0.011$, $p = 0.99$). (**F**) Representative EEG recordings and Fast Fourier Transform (FFT) power spectrum of non-fatal seizure in a Depdc5$^{c/-}$ mouse, followed with a 3 min 34 s postictal generalized EEG suppression (PGES). The color-coded FFT power spectrum shows EEG amplitude and frequency changes from motor cortex (M1) and hippocampus (Hip). (**G**) Representative EEG recordings and FFT of a fatal seizure in a Depdc5$^{c/-}$ mouse terminating with hind limb extension and prolonged PGES. (**H**) Duration of tonic, clonic and wild running (WR) phases during non-fatal and fatal seizures in Depdc5$^{c/-}$ mouse (n=5-12, Two-way ANOVA revealed main effect of behavior type, $F_{2,45}=62.85$, $p<0.0003$; and main effect of interaction, $F_{2,45}=9.98$, $p=0.0003$; Bonferroni's post-hoc tests). (**I**) Duration of wild running in non-fatal and fatal seizures (n=5-21, unpaired t-test, $t_{24} = 3.83$, $p = 0.0012$). Results are given as mean ± SEM. *$p < 0.05$, **$p < 0.01$, ***$p < 0.001$ vs. *Depdc5*$^{+/+}$.

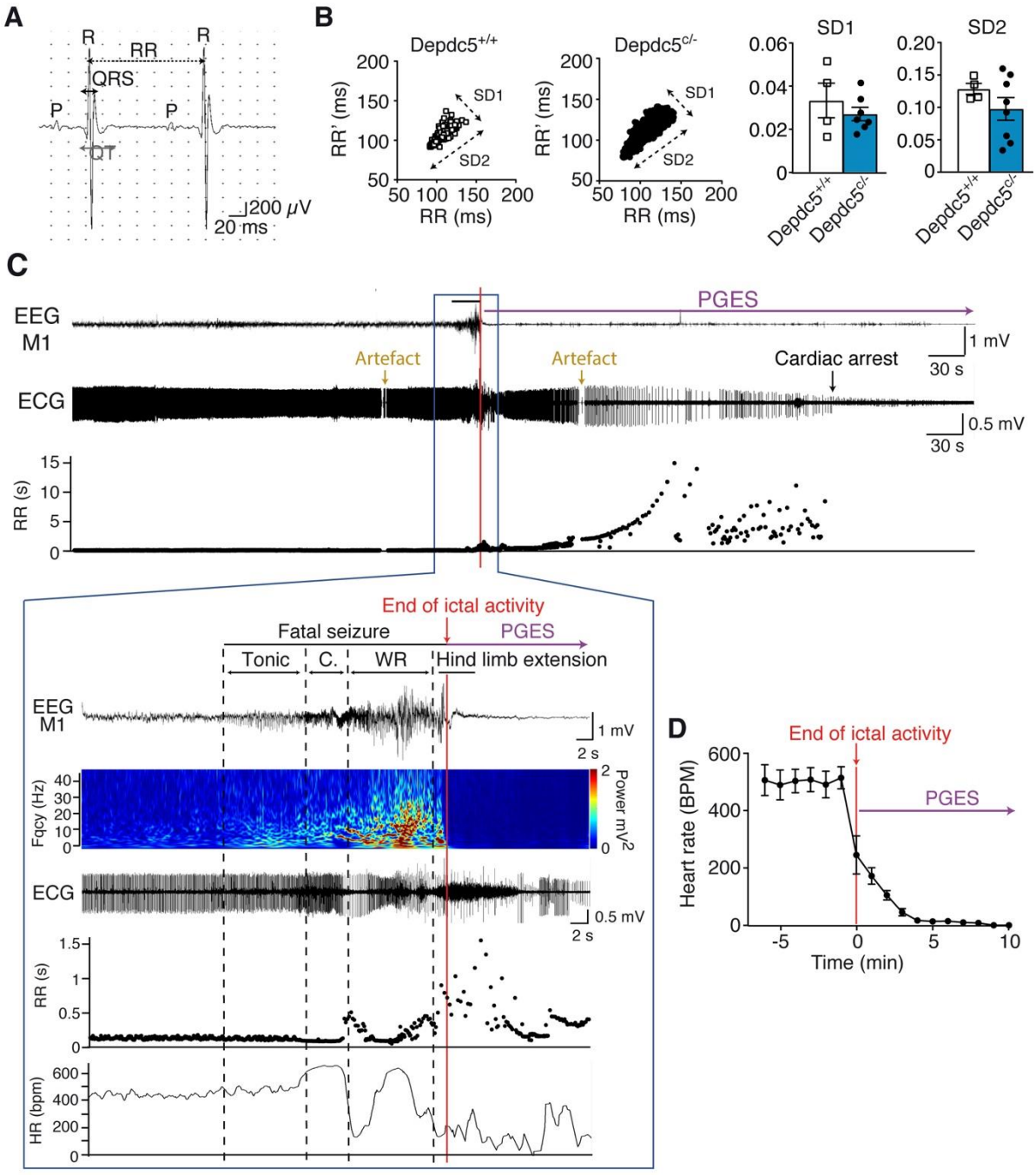

Figure 4. EEG-ECG records from *Depdc5*$^{c/-}$ mice at rest and during a spontaneous fatal seizure. (**A**) Example of ECG records in anesthetized mice (**B**) *In vivo* recordings of heart rate variability is represented with Poincaré plots in *Depdc5*$^{c/-}$ and *Depdc5*$^{+/+}$ mice, and quantified by SD1 (Mann-Whitney, U=7, p=0.53) and SD2 (Mann-Whitney, U=11, p=0.46) parameters (n=4-8 mice, N > 500 RR measures per animal). (**C**) Representative simultaneous EEG-ECG records and RR plot before, during and after a fatal seizure in *Depdc5*$^{c/-}$ mouse, terminating with prolonged postictal generalized EEG suppression (PGES). Fast Fourier Transform power spectrum shows EEG amplitude and frequency changes from motor cortex (M1). Dashed lines indicate

the beginning of the phase indicated by the label (Tonic; C: clonic and WR: Wild running). RR length and heart rate (mean number of RR in 2s) changed after the beginning of the seizure, during the clonic phase. The ECG during the seizure and after the hind limb extension phase is partially obscured by electrical activity of muscle contraction. Artifacted RR measures were excluded. (**D**) Average heart rate changes during and after the seizure in six *Depdc5*$^{c/-}$ mice. Results are mean ± SEM.

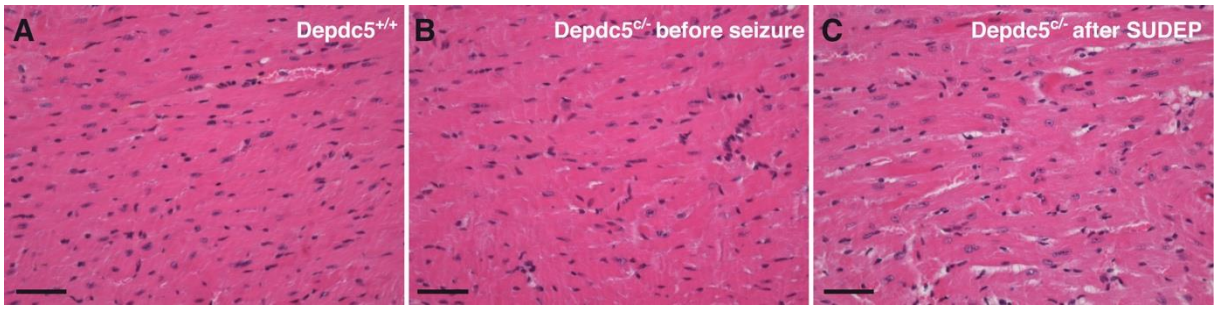

Figure 5. Mouse heart histology before and after SUDEP-like event. (**A-C**) Hematoxylin and eosin (H&E) stained transversal sections of the anterior interventricular artery in a control *Depdc5*$^{+/+}$ (**A**), *Depdc5*$^{c/-}$ before seizure (**B**) and *Depdc5*$^{c/-}$ after SUDEP-like event (**C**). No contraction band necrosis nor fibrosis were detected in *Depdc5*$^{c/-}$ heart after SUDEP. Scale bars represent 100 µm (**A**-**C**).